LLNL-JRNL-2006886

Lawrence Livermore National Laboratory

A Novel Microstructural Approach for TRIP/TWIP β-Ti Alloys Using Intermetallic Precipitation

B Ellyson, J Almer, J Park, C Rietema, N Peterson, K Clarke, A Clarke

July 2025

Disclaimer

This work performed under the auspices of the U.S. Department of Energy by Lawrence Livermore National Laboratory under Contract DE-AC52-07NA27344.

A Novel Microstructural Approach for TRIP/TWIP β-Ti Alloys Using Intermetallic Precipitation

Prepared for submission to Materials Science and Engineering A

25th of March, 2025

Benjamin Ellyson[a,d], Connor J. Rietema[a,d], Nathan E. Peterson[b,d], Valava S. Rani[a], Jun-Sang Park[c], Jon Almer[c], Kester Clarke[b,d], Amy J. Clarke[b,d]

a Materials Science Division, Lawrence Livermore National Laboratory, Livermore, CA, 94450, USA

b Sigma Manufacturing Sciences Division, Los Alamos National Laboratory, Los Alamos, NM, 87545, USA

c Advanced Photon Source, Argonne National Laboratory, Argonne, IL, 60439, USA

d Department of Metallurgical and Materials Engineering, Colorado School of Mines, Golden, CO, 80401, USA

Abstract

Interest in metastable β-Ti has grown, due to the exceptional work hardening caused by TRansformation and TWinning Induced Plasticity (TRIP/TWIP). A current challenge is increasing the yield strength, while maintaining the benefits of TRIP/TWIP. This study presents the first report of TRIP/TWIP in a metastable β-Ti alloy containing intermetallic compounds, specifically Ti silicide precipitates. Silicon (Si) additions enable the formation of silicide particles, which can be precipitated, dissolved, and controlled through tailored heat treatments. In-situ synchrotron x-ray diffraction during tensile testing reveals primary {332}<113> twinning activates first, followed by TRIP, leading to extensive work hardening and uniform elongation in the solutionized state. These findings open a novel microstructural approach to the design of multiphase TRIP/TWIP titanium alloys, relying on intermetallic precipitation rather than allotropes such as α or ω phase, and lay the groundwork for future studies on intermetallic precipitation strengthening.

Introduction

Titanium alloys have long been a cornerstone of aerospace and biomedical applications due to their exceptional mechanical properties, including high strength-to-weight ratios. Conventional titanium alloys typically rely on multiphase microstructures involving alpha (α)- and beta (β)-phase allotropes, with the α phase providing strength at the expense of ductility [1]. Metastable β-Ti alloys, however, offer a unique advantage: the low β-phase stability enables deformation mechanisms such as TRansformation Induced Plasticity (TRIP) and TWinning Induced Plasticity (TWIP), which result in high work hardening rates (WHRs) and uniform elongations [2,3]. These mechanisms make TRIP/TWIP β-Ti alloys attractive candidates for lightweight, damage-tolerant applications.

Despite their promise, TRIP/TWIP β-Ti alloys have been hindered by relatively low yield strengths. Recent efforts to address this issue have focused on multiphase microstructures that incorporate secondary phases while preserving TRIP/TWIP activity in the β matrix. Previous studies have explored β+α [3,4,5] and β+ω [6,7,8] microstructures, but these approaches rely exclusively on precipitation of titanium allotropes.

To date, no studies have investigated the use of intermetallic compounds as a secondary phase in TRIP/TWIP-active β-Ti alloys.

This study introduces a novel microstructural strategy for TRIP/TWIP-active β-Ti alloys by incorporating Ti silicide intermetallic compounds as a secondary phase. Si was selected as the intermetallic-forming solute for multiple reasons. Ti alloys containing Si are known to form Ti silicide intermetallics. Silicide-reinforced Ti alloys have previously been studied for high-temperature strength and creep resistance [9]. Si also allows for significant precipitation with dilute additions, allowing for large variations in volume fraction of silicides with minor changes in composition of the β-phase matrix. This factor is crucial, since the chemical composition of the β-phase is the prime factor in controlling the propensity for TRIP and/or TWIP [10]. However, the effect of Si solute additions on TRIP/TWIP behavior is not well understood and requires further investigation.

Here we investigate the feasibility of this approach by addressing three key questions: 1. Understanding Si supersaturation effects on TRIP/TWIP and microstructural evolution of the β-phase during deformation. 2. Whether alloy composition changes and heat-treatments can be utilized to control silicide precipitation and dissolution. 3. If TRIP/TWIP remains active in a metastable β phase that also contains silicide particles.

Our findings show that each of these three requirements is met and demonstrate that TRIP/TWIP mechanisms remain active in β + silicide microstructures, proving the feasibility of this novel approach. This work represents the first report of TRIP/TWIP activity in a metastable β-Ti alloy containing intermetallic compounds, rather than titanium allotropes, opening a new pathway for designing advanced multiphase TRIP/TWIP alloys.

Methods

The alloys were produced by arc melting Ti, Cr, Al, Mo and Si in argon and were remelted 4 times to mitigate elemental segregation. The buttons were forged at 1200 °C to 9.5 mm square cross-sections, then hot-rolled to 2.5 mm at 1000 °C. Specimens produced from the hot rolled strips were encapsulated in quartz tubes and solution treated at 750, 820, 910 and 1000 °C for 1 h, followed by quenching in water to produce different volume fractions of precipitates. Tensile specimens were machined with a 15 mm gage length and 3.5 by 2.3 mm gage cross-section. Electron back scatter diffraction (EBSD) specimens were prepared by electropolishing in a solution of perchloric, hydrochloric acid in methanol. EBSD was conducted on a Helios FIB/SEM at a voltage of 20 kV, a current of 11 nA and a 0.5 µm step size. In-situ synchrotron x-ray diffraction (XRD) experiments were conducted at beamline 1-ID at the Advanced Photon Source at Argonne National Laboratory. The incident X-ray energy was 71.6 KeV. The beam was collimated to 0.2 mm square. The measurements were performed in Debye-Scherrer geometry, with the detector array placed 2 m from the sample. The tensile specimens were tested at a strain rate of 10^{-4} s^{-1} to failure, during which continuous diffraction measurements (0.1 s exposure time) were made. Measurements were taken in a 1x3 grid (0.2 mm apart) transverse to loading to increase grain sampling during continuous acquisition. The data collected at each exposure was azimuthally integrated using GSAS-II and each set of three measurements was summed to increase grain statistics. Complementary mechanical testing was conducted on an electro-mechanical load frame at a strain rate of 10^{-3} s^{-1} using a 25 mm extensometer.

Results and Discussion

Two alloys were designed for this study. Ti-8Cr-1.5Al-0.5Si (Ti-81505) (wt. %, unless otherwise stated) was designed as a control alloy to compare with an alloy published by Brozek et al. [11]. Ti-6Cr-5Mo-0.5Si (Ti-6505) was designed as a novel composition based on the Ti-Cr-Mo system reported by Gao et al. [12]. The compositions were designed using the d-electron method [13], in combination with thermodynamic simulations by CALPHAD, to obtain TRIP/TWIP-capable alloys and suitable phase fields for silicide precipitation and dissolution. The bond order (B_o) and mean d-orbital energy (M_d) positions of the two alloys are shown in Supplementary Figure S1. Pseudo-binary phase diagrams were used to determine the silicide solvus. Figure 1 shows the calculated phase diagrams with the 0.5% Si line indicated. Samples of Ti-81505 and Ti-6505 were solution heat treated at selected temperatures of 750, 820 and 910 °C for 1 h to show that silicide content could be controlled. Figure 1 shows optical micrographs corresponding to each alloy at each temperature. Notably, the Ti-81505 sample solution treated at 910 °C shows complete dissolution of secondary particles, in agreement with thermodynamic predictions. Energy dispersive spectroscopy (EDS) was performed on samples solution treated at 820 °C to confirm that secondary particles are silicides, as shown in Supplementary Figure S2 for Ti-6505. Solution treatment temperatures of 910 and 1000 °C were sufficient to dissolve the silicides in Ti-81505 and Ti-6505, respectively. Interestingly, the dissolution of silicides at 1000 °C presents a disagreement with the phase diagram calculated for Ti-6505, which may indicate the curvature of the silicide solvus is more pronounced than predicted in Figure 1.

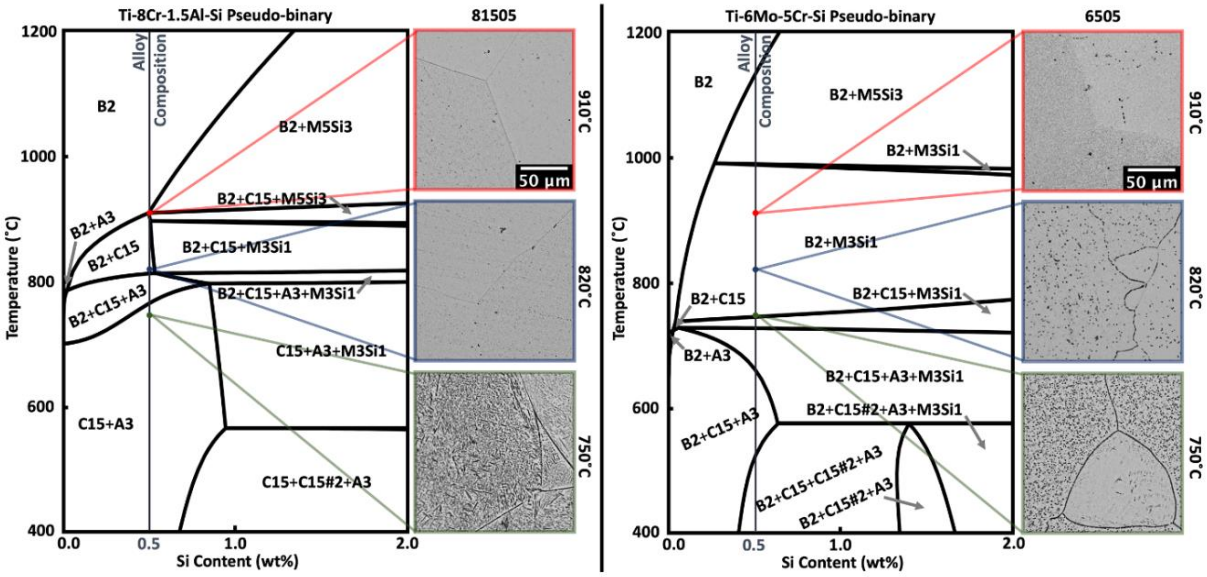

Figure 1. Pseudo-binary phases diagrams for Ti-8Cr-1.5Al-XSi and Ti-6Cr-5Mo-XSi alloys and corresponding light optical micrographs for the solution treatment temperatures indicated for 1 h.

After solution treatment above the silicide solvus, cold-rolling to 5% reduction was performed to identify the active deformation mechanism(s) in a microstructural condition of Si-supersaturated β-phase without silicide particles. EBSD scans of cold rolled Ti-81505 and Ti-6505 are shown in Figure 2. Both scans show {332}<113> deformation twinning (TWIP) and α" transformation (TRIP), validating the alloy design. Interestingly, both alloys also exhibit secondary transformation operating within primary {332}<113> twins.

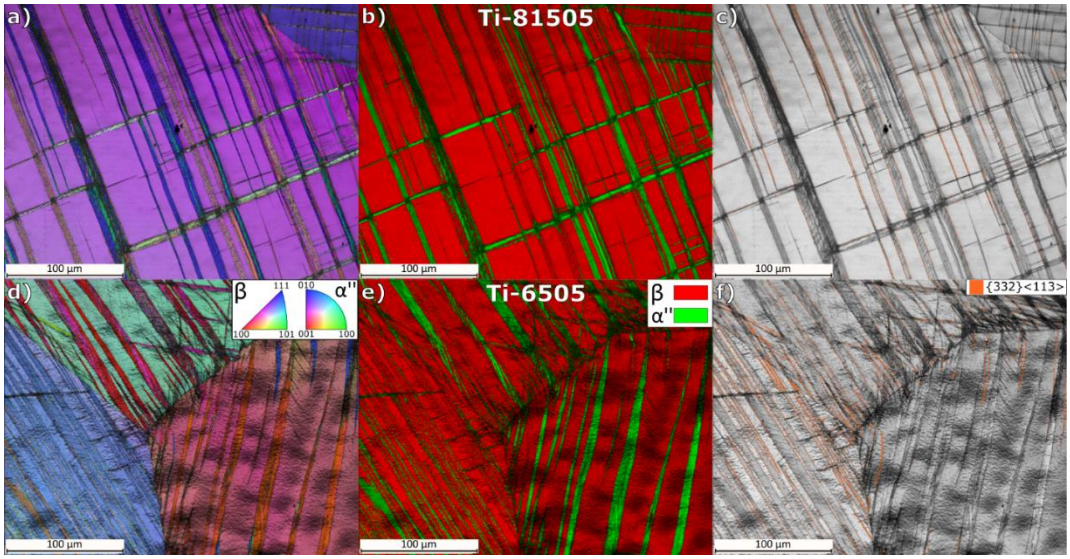

Figure 2. EBSD scans of solutionized a)-c) Ti-8505 and d)-f) Ti-6505 cold rolled to 5% total reduction from the β-solutionized state. a) and d) are inverse pole figure (IPF)+image quality (IQ) maps, b) and e) are phase + IQ maps, and c) and f) are IQ maps with {332}<113> twin boundary overlays.

Bulk tensile tests were performed on samples solution treated at 1000 °C for 1 h then water quenched, generating a Si-supersaturated β-phase microstructure without silicides (Figure 3). Both alloys exhibit high uniform elongations and WHRs expected for TRIP/TWIP β-Ti alloys. Yield strengths of roughly 500 MPa and 440 MPa and uniform elongations of 39% and 37%, respectively, for Ti-81505 and Ti-6505 were obtained. The true ultimate tensile strengths of both alloys are comparable at ~1100 MPa. Ti-81505 exhibits nearly identical tensile behavior to the baseline alloy Ti-8.5Cr-1.5Al reported by Brozek et al. [10] (Supplementary Figure S3). The similarity between Ti-8.5Cr-1.5Al and Ti-81505 indicates that dilute Si additions do not significantly impact the mechanical properties of metastable β-Ti alloys. This result is encouraging for the future design of silicide-containing microstructures, as solution and precipitation treatments will cause a variation of the Si content remaining in solution in the β phase. Differences in yield stresses are most likely due to differences in processing history, leading to grain size differences.

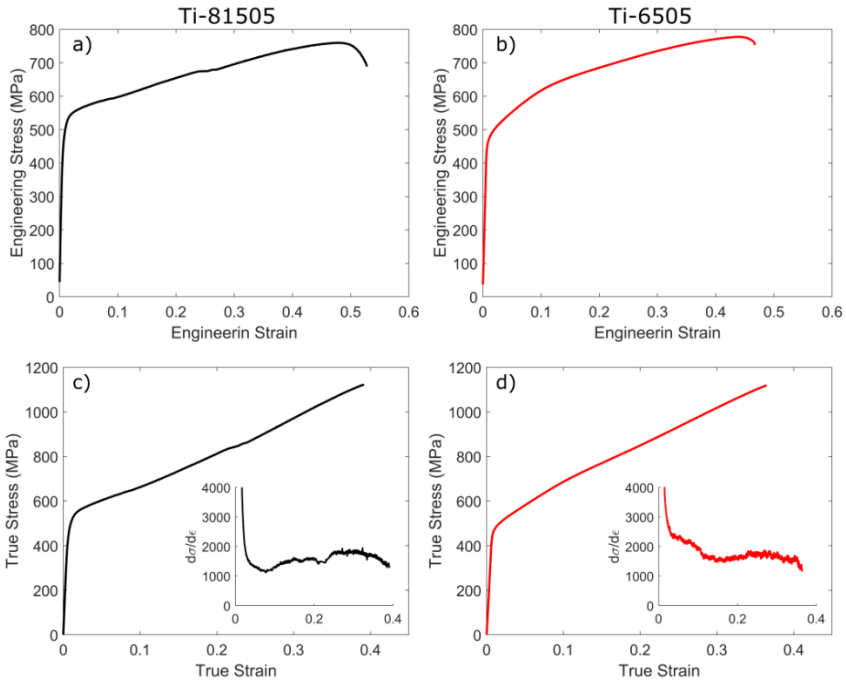

Figure 3. Mechanical behavior of Ti-81505 and Ti-6505 alloys solution treated for 1 h at 1000 °C then water quenched. Engineering stress versus engineering strain curves for a) Ti-81505 and b) Ti-6505. True stress versus true strain curves for c) Ti-81505 and d) Ti-6505. Instantaneous WHRs are shown as insets in c) and d).

In-situ synchrotron XRD during tensile testing was also performed on Ti-81505 and Ti-6505 alloys to elucidate the activation sequence of deformation mechanisms in the single β-phase condition. Results for Ti81505 are not presented for brevity. Results from Ti-6505 are presented in Figure 4. Figure 5 a) shows engineering stress versus engineering strain, with each diffraction frame indicated by square markers. The stress/strain response is comparable to the bulk test conducted with an extensometer in Figure 4 a), but differences are present. The yield stress, total elongation and ultimate tensile stress are higher than those for the ex-situ, bulk tensile testing shown in Figure 3 a). The difference in mechanical properties is perhaps due to grain size relative to the gage section dimensions of the smaller specimens used in the in-situ tests, or due to low-temperature aging [6] that occurred during transport to the synchrotron facility. The in-situ tension specimens had a smaller cross-section containing a dozen or less grains, which can affect elongation. Figure 4 b) shows a waterfall plot of XRD patterns from selected strain levels. The first frame at the onset of elasto-plastic transition (0.03 strain) shows characteristic signs of as-quenched β+ω microstructures. Three major β peaks are indicated by blue triangles. The next frame at 0.05 strain shows the first signs of martensite, indicating TRIP, which coincides with yielding. The highest intensity martensite peak is indicated with a green diamond. The next two frames at 0.098 and 0.17 strain show the major β-phase peaks decrease, while martensite peaks increase. This change in relative intensity is indicative of TRIP progressing with plastic strain. The last two frames at strain levels of 0.26 and 0.38 show relative intensities shifting to the lower index peaks in both the β and α" martensite phase. This change in relative intensity shows texture is evolving within each phase as the capacity for transformation is exhausted and plasticity is mediated by twinning and slip in both phases. A more precise picture of the sequence of deformation mechanism activation can be constructed by looking at specific peaks of the β and α" phases.

This is necessary because of overlap in higher intensity reflections caused by closely related crystal symmetries of the β and α" phases. Figure 4 c) shows an integrated heatmap of intensity versus 2θ and engineering strain for isolated neighboring peaks: β_{200}, α''_{022} and α''_{112}. Figure 4 d) shows the integrated intensity of each peak as a function of engineering strain. The integrated intensity was obtained by peak-fitting each peak in each frame. The integrated intensity of the β_{200} increases first as yielding begins. The martensite peaks, α''_{022} and α''_{112}, start gaining in intensity after a few frames around 0.06 strain. This indicates twinning activates in the β matrix first before TRIP begins. TRIP starts to occur soon afterwards at 0.06 strain, where all three peaks increase in intensity, indicating simultaneous β-phase TWIP and β to α" TRIP. Once 0.12 strain is reached, the β_{200} integrated intensity starts to decrease, while α''_{022} and α''_{112} peaks continue to gain in integrated intensity as TRIP consumes more β phase. At 0.2 strain, the α''_{022} peak reaches a maximum, which coincides with the minimum intensity of the β_{200} peak, while the

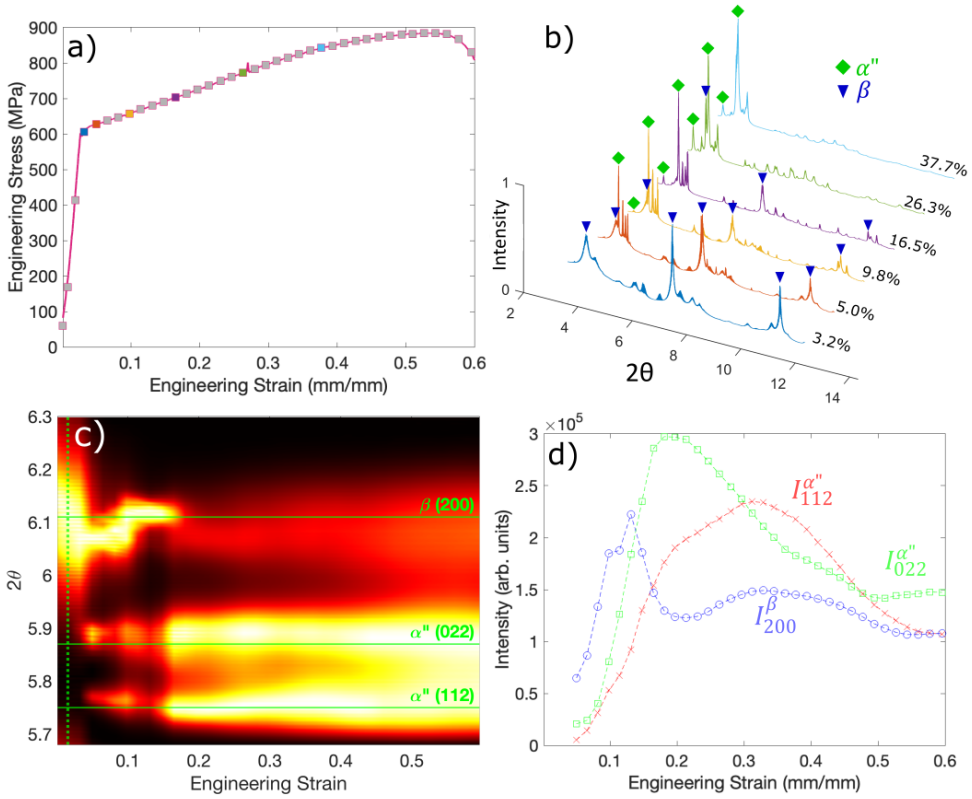

Figure 4. Synchrotron XRD results from an in-situ tensile test of Ti-6505. a) Engineering stress versus engineering strain curve, showing the stress and strain values for every diffraction frame. The mechanical data has been compliance corrected. b) Waterfall plot showing integrated diffraction patterns for the whole 2θ range at the indicated strains. Only major peaks of interest are indicated for clarity (all peaks are not provided here). The frames are indicated by markers filled with the same color as the line in a). c) An integrated diffraction heat map showing the evolution of the intensities of three peaks β_{200}, α''_{022} and α''_{112} of interest during the early stage of tensile deformation. d) Integrated intensity of the three diffraction peaks shown in c) as a function of engineering strain.

α''_{112} continues to increase more slowly. These changes in trends are indicative of transformation reaching the maximum extent and plasticity operating thereafter by TWIP and slip. Specifically, the decrease in intensity of α''_{022} while α''_{112} increases at a slower rate implies a change in texture within the martensite,

an indicator of twinning and slip. All three peaks diminish in intensity after 0.31 strain, since texturing from continued TWIP and slip continues to shift intensities towards lower index peaks.

The tensile testing (Figure 3), in-situ synchrotron XRD (Figure 3) and EBSD post-mortem characterization (Figure 2) support the validity of the d-electron alloy design in predicting TRIP/TWIP behavior in Si containing metastable β-Ti alloys. Furthermore, the comparison of the Ti-81505 and Ti-8.5Cr-1.5Al reported by Brozek et al. [10] supports the conclusion that dilute additions of Si do not strongly alter the mechanical behavior of TRIP/TWIP metastable β-Ti alloys. This finding is paramount in supporting the development of silicide containing microstructures, as the Si content will vary as a function of silicide precipitation. The single β-phase state represents a bounding upper condition, since all the Si is in solution in the β-phase. The in-situ synchrotron XRD data show primary {332}<113> twinning activates as the first deformation mechanism after the onset of yield, followed by the activation of TRIP (Figure 5), as for Ti-12Mo [14]. Further plastic strain accumulation results in the activation of secondary TRIP and TWIP within the primary twins and the matrix of the β grains (Figure 2). The yield stresses of the two alloys reported herein, namely Ti-81505 and Ti-6505, are also comparable to other TRIP/TWIP β-Ti alloys like Ti-12Mo, [2], Ti-8.5Cr-1.5Al [10], and Ti-9Mo-6W (wt.%) [15]. While the yield stress is lower than more recent TRIP/TWIP alloys, such as Ti-7Cr-3Mo (wt.%) [12] and multi-modal TWIP alloys, such as Ti-4Cr-3Mo-1Fe (wt.%) [16], the lower yield stress shown in the single β-phase state provides an opportunity to investigate the potential strengthening obtained from controlled precipitation of silicides in the β phase matrix. Furthermore, the microstructural development study presented in Figure 1 shows that silicides can precipitate or dissolve by selecting the appropriate temperature, which supports the conclusion that silicide precipitation can be tailored by appropriate processing pathways.

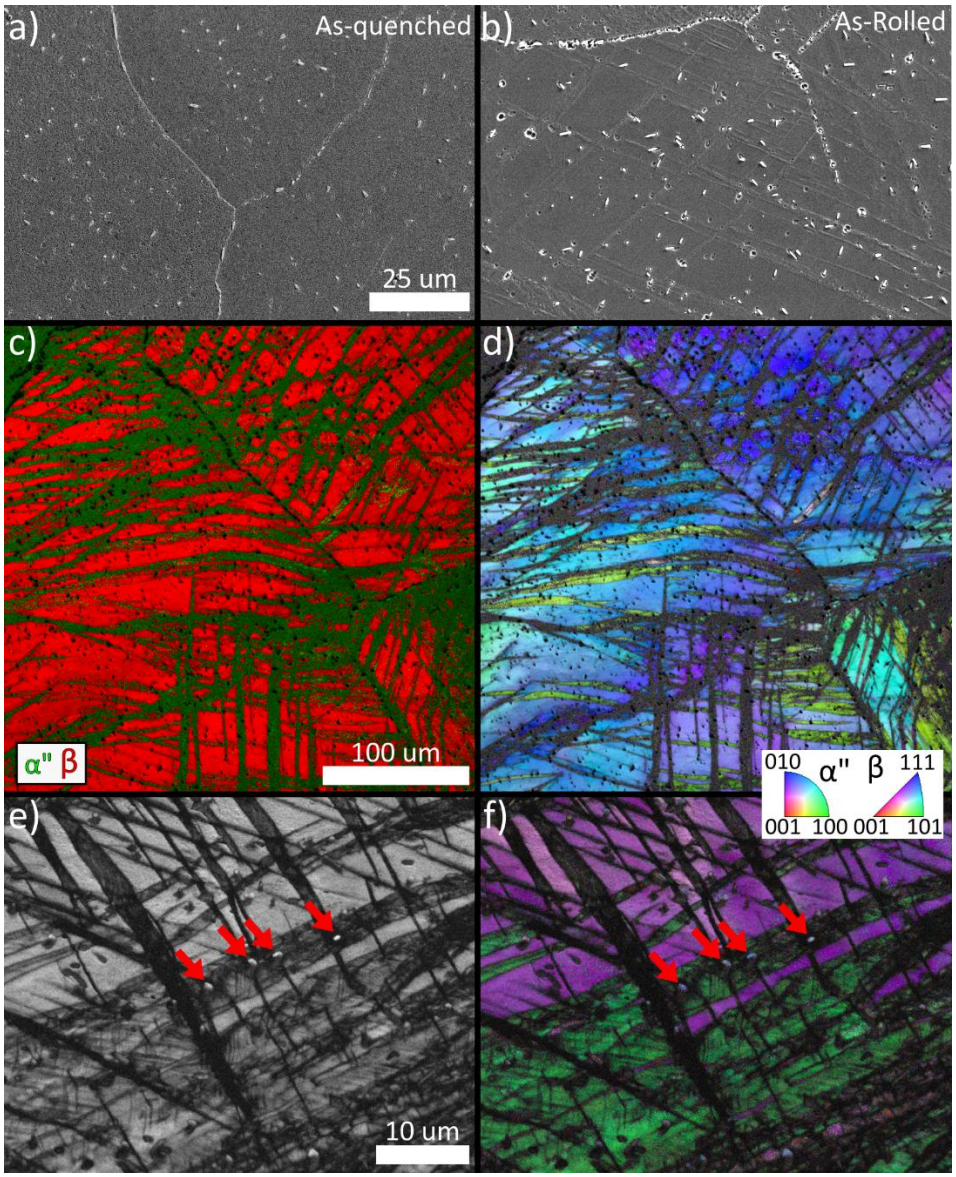

Figure 5. SEM micrographs and EBSD scans of Ti-6505 in the 820C WQ in as-quenched (a) and cold-rolled state (b-f). a) SEM micrograph of the Ti-6505 alloys in the 820C WQ condition before cold rolling, showing silicide particles in the β grains and on the grain boundaries. B) SEM micrograph of the Ti-6505 in 820C WQ condition after 5% cold rolling showing transformation product and silicide particles. b) Phase +IQ maps of and EBSD scan of the same condition shown in b). d) IPF+IQ map of the same EBSD scan shown in c). e) IQ map of a higher magnification EBSD scan of the same condition shown in b, c and d). f) IPF+IQ map of the same EBSD scan shown in e). The red arrows in e) and f) highlight silicide particles that exist within a transformation band, other particles are also visible but not indicated by arrows.

The final part of proving the feasibility of the proposed approach lies in the activation of TRIP and TWIP during deformation in a β + silicide microstructural condition. To demonstrate this, samples of Ti-6505 were solution treated at 820 °C for 1 h then water quenched to form a metastable β phase microstructure that contains silicide particles as shown in Figure 1. Figure 5 shows SEM micrographs and EBSD scans

before and after cold rolling Ti-6505 solution treated at 820 °C. Silicides are dispersed within the β grains and at the grain boundaries prior to deformation (Figure 5 a)). This sample was cold rolled to 5 % reduction to demonstrate that TRIP/TWIP is active in the β + silicide condition. After cold rolling, deformation product is visible within the β grains along with silicides (Figure 5 b)). EBSD scans of the cold-rolled condition shows that the deformation products are indexed as α" martensite (Figure 5c)). It is likely that some of these deformation bands initially formed as twins and were internally populated by secondary TRIP. The deformation product can be seen to be wavier, shorter, and generally more complex as compared to the nominally straight bands exhibited by the single phase β microstructures without silicides (Figure 2)) for the same amount of cold rolling reduction. This is most likely due to the interaction between TRIP/TWIP forming in the presence of the silicide particles. Figure 5 e) and 5 f) show a higher magnification EBSD scan of the same sample where silicide particles can be seen to co-exist with the deformation product. Red arrows in Figure 5 e) and 5 f) highlight silicide particles contained within a large band and at the intersection between different variants of deformation product. The exact nature and mechanisms of the interaction between the silicide particles and the twin and martensite bands is complex and requires further study. Fine-scale characterization of interactions between silicides and deformation products is outside the scope of the current work, but will be the subject of a follow-on study. Nevertheless, the results presented in Figure 5 prove the feasibility of TRIP/TWIP activity during deformation of a metastable β-phase that contains silicide particles.

The next step in the development of intermetallic strengthened, metastable β-Ti alloys requires understanding how to control the volume fraction, distribution, and morphology of the silicide particles in the β-phase matrix and the impacts to strength and work hardening. Previous work published on conventional silicide-reinforced Ti alloys has shown that grain boundary silicides can be efficient pinning centers for controlling grain growth during thermo-mechanical processing [9]. Secondary silicide precipitation can also be used to tailor the size distribution of the precipitates to create refined particles more efficient at strengthening the matrix. The strategy of designing a two-scale architecture of silicides in a β-Ti matrix has been shown to lead to strengthening by Jiang et al. [17]. While Jiang et al.'s work proves the possibility of tailoring silicide precipitation to form nano-scale precipitates, the β-phase in their $Ti_{70}Nb_{10}Mo_{10}Zr_{10}$ (at. %) base-alloy is stable and does not exhibit any TRIP/TWIP behavior. As such, it is feasible to consider multi-stage thermo-mechanical processing pathways to tailor β grain size, grain boundary, and intragranular silicide content and size. The possibility of combining silicide strengthening with other phases, such as the α phase or ω phase, also exists. Current work is underway to develop and understand thermo-mechanical processing pathways to control silicide precipitation for β grain size control and strengthening and will be the subject of a follow-on publication.

Conclusion

This study introduces a novel microstructural strategy for the design of TRIP/TWIP-active beta titanium (β-Ti) alloys by incorporating intermetallic compounds, specifically Ti silicides, as a secondary phase. By using a combination of thermodynamic simulations and d-electron alloy design, TRIP/TWIP active, metastable β-Ti alloys with Si additions were produced. Two alloys were designed and studied, namely Ti-8Cr-1.5Al-0.5Si and Ti-6Cr-5Mo-0.5Si (wt.%). Solution temperatures selected by thermodynamic simulations showed that silicide content can be controlled and dissolved. The strategy of designing TRIP/TWIP active, β-Ti alloys that contain silicides or not was also proven through post-mortem characterization of cold-rolled samples. Si supersaturation in the TRIP/TWIP active β phase does not strongly affect microstructural evolution and

mechanical properties, and the sequence of deformation mechanisms was identified by in-situ synchrotron XRD during quasi-static tensile deformation. The results presented here prove that dilute Si additions can be used to form silicide precipitates, while maintaining TRIP/TWIP activity in the β-phase matrix. To the authors' knowledge, this represents the first report of TRIP/TWIP-active alloys with Si additions and/or secondary intermetallic particles, rather than precipitates of Ti allotropes (such as α- or ω-phase), opening the way to a completely novel strengthening pathway for TRIP/TWIP β-Ti alloys.

Acknowledgements

This work was supported by the Department of the Navy, Office of Naval Research under award No. N00014-18-1-2567. Any opinions, findings, and conclusions or recommendations expressed in this material are those of the author(s) and do not necessarily reflect the views of the Office of Naval research. The Tescan instrument used for this work was acquired through the support of the National Science Foundation (DMR-1828454). This research used resources of the Advanced Photon Source, a U.S. Department of Energy (DOE) Office of Science User Facility operated for the Office of Science by Argonne National Laboratory under contract no. DE-AC02-06CH11357. Preparation of this manuscript (BE and CJR) was performed under the auspices of the U.S. Department of Energy by Lawrence Livermore National Laboratory under contract No. DE-AC52-07NA27344. NEP, AJC, and KDC acknowledge support by the U.S. Department of Energy through the Los Alamos National Laboratory during the preparation of this manuscript. Los Alamos National Laboratory is operated by Triad National Security, LLC, for the National Nuclear Security Administration of U.S. Department of Energy (Contract No. 89233218CNA000001).

Data availibility

Data will be made available on request

CrediT authorship contribution statement

B. Ellyson: Writing - original draft, Investigation, Formal analysis, Conceptualization **C.J Rietema:** Investigation, **N.E. Peterson**: Formal analysis, **V.S. Rani**: Investigation, **J.S. Park**: Investigation, **J. Almer**: investigation, **K.D. Clarke**: Investigation, Writing – review and editing, **A.J. Clarke**: writing – review and editing, Project administration, Funding acquisition, Conceptualization.

References

[1] Donachie MJ. "Titanium: a technical guide", ASM International; 2000.
[2] Marteleur M, Sun F, Gloriant T, Vermaut P, Jacques PJ, Prima F. "On the design of new β-metastable Ti alloys with improved work hardening rate thanks to simultaneous TRIPand TWIP effects", *Scripta Materialia*, 2012; 66(10):749-52.
[3] Min X, Chen X, Emura S, Tsuchiya K. "Mechanism of twinning-induced plasticity in β-type Ti-15Mo alloy", *Scripta Materialia*, 2013; 69(5):393-6.
[3] Danard Y, Poulain R, Garcia M, Guillou R, Thiaudière D, Mantri S, et al. "Microstructure Design and in-situ investigation of TRIP/TWIP effects in a forged dual-phase Ti–10V–2Fe–3Al alloy", *Materialia*. 2019; 8:100507.
[4] Lilensten L, Danard Y, Poulain R, Guillou R, Joubert JM, Perrière L, et al. "From single phase to dual-phase TRIP-TWIP Ti alloys: Design approach and properties", *Materialia*. 2020; 12:100700.
[5] Zhu C, Zhang Xy, Li C, Liu C, Zhou K. "A strengthening strategy for metastable β Ti alloys: Synergy effect of primary α phase and β phase stability", *Materials Science and Engineering: A*. 2022; 852:143736.

[6] Sun F, Zhang J, Vermaut P, Choudhuri D, Alam T, Mantri S, et al. “Strengthening strategy for a ductile metastable β-Ti alloy using low-temperature aging”, *Materials Research Letters*. 2017; 5(8):547-53.
[7] Ellyson, Benjamin, et al. "Tuning the strength and ductility balance of a TRIP titanium alloy." *Scripta Materialia* 194 (2021): 113641
[8] Qian, Bingnan, et al. "Mechanisms underlying enhanced strength-ductility combinations in TRIP/TWIP Ti-12Mo alloy engineered via isothermal omega precipitation." *Acta Materialia* 245 (2023): 118619.
[9] Zhao, Ertuan, Shichen Sun, and Yu Zhang. "Recent advances in silicon containing high temperature titanium alloys." *Journal of Materials Research and Technology* 14 (2021): 3029-3042.
[10] Castany, Philippe, et al. "Design of strain-transformable titanium alloys." *Comptes Rendus. Physique* 19.8 (2018): 710-720.
[11] Brozek, C., et al. "A β-titanium alloy with extra high strain-hardening rate: design and mechanical properties." *Scripta Materialia* 114 (2016): 60-64.
[12] Gao, Junheng, et al. "Deformation mechanisms in a metastable beta titanium twinning induced plasticity alloy with high yield strength and high strain hardening rate." *Acta Materialia* 152 (2018): 301-314.
[13] Abdel-Hady, Mohamed, Keita Hinoshita, and Masahiko Morinaga. "General approach to phase stability and elastic properties of β-type Ti-alloys using electronic parameters." *Scripta Materialia* 55.5 (2006): 477-480.
[14] Sun, F., et al. "Investigation of early stage deformation mechanisms in a metastable β titanium alloy showing combined twinning-induced plasticity and transformation-induced plasticity effects." *Acta Materialia* 61.17 (2013): 6406-6417.
[15] Sun, F., et al. "A new titanium alloy with a combination of high strength, high strain hardening and improved ductility." *Scripta Materialia* 94 (2015): 17-20.
[16] Ren, Lei, et al. "Simultaneously enhanced strength and ductility in a metastable β-Ti alloy by stress-induced hierarchical twin structure." *Scripta Materialia* 184 (2020): 6-11.
[17] Jiang, Shan, et al. "Significantly strengthening the Ti70Nb10Mo10Zr10 alloy via architecting two-scale silicide reinforcements." *Journal of Alloys and Compounds* 835 (2020): 155255.

Supplementary Materials

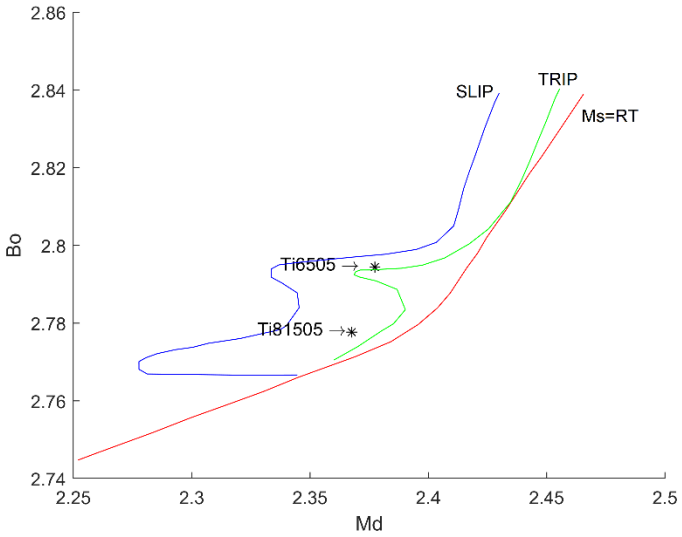

Figure S1. A Bo-Md map showing the position of the two newly designed silicon (Si)-containing alloys. Both compositions assume the β phase exhibiting complete dissolution of Si into the β matrix.

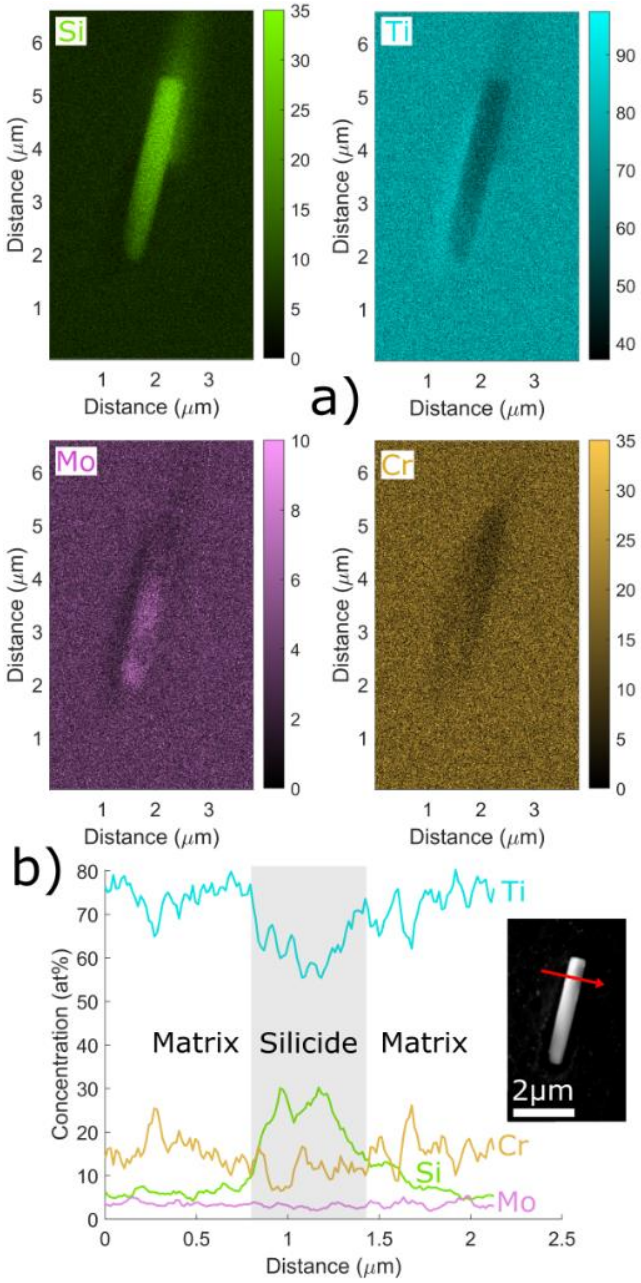

Figure S2. EDS map of a Ti silicide particle taken from the Ti-6505 alloy solution treated at 820 °C for 1 h. a) Chemical maps showing the distribution of solute elements in the matrix and a representative silicide particle. b) A linescan taken from the EDS map showing the concentration (at. %) of solute elements across the particle. The inset image shows the location of the linescan relative to the precipitate.

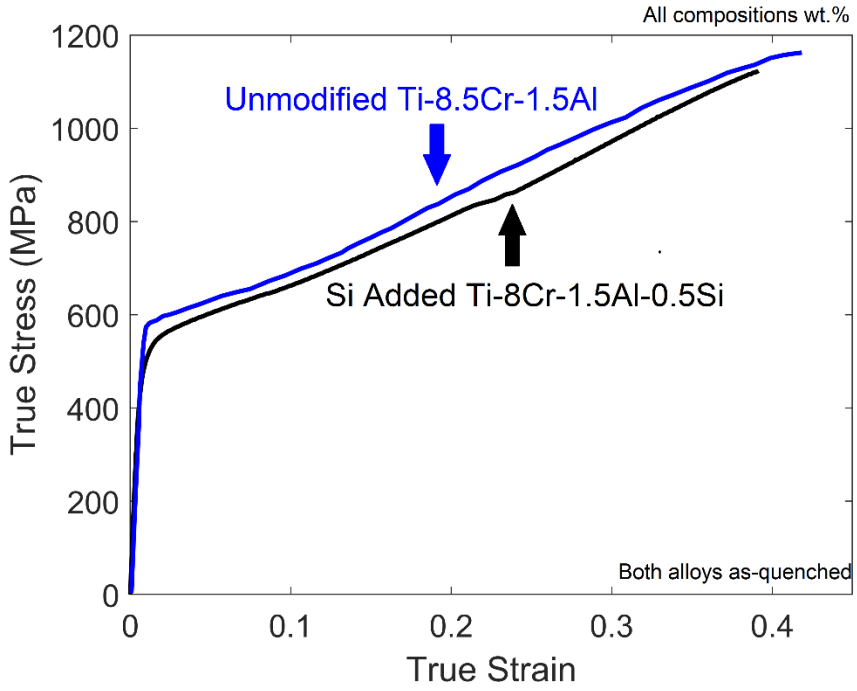

Figure S3. True stress versus true strain curves of Ti-81505 compared to Ti-8Cr-1.5Al. Data for Ti-8.5Cr-1.5Al taken from [11]. It should be noted that both alloys exhibited differences in processing history and grain size, although both were tested in a β+ω condition.